

Review of General Modeling Approaches of Power Converters*

Dong Yan¹, Chenglin Yang², Lijun Hang^{1*}, Yuanbin He¹, Ping Luo¹, Lei Shen¹ and Pingliang Zeng¹

(1. Department of Electrical Engineering, Hangzhou Dianzi University, Hangzhou 310000, China;

2. INVT Power System(Shenzhen)Co., Ltd., Shenzhen 518055, China)

Abstract: The modeling approaches of power converters occupy an important position in power electronic systems and have made considerable progress over the past years. Continuous modeling approaches and linearization techniques are reviewed, including the state-space average model, generalized average model, averaged small-signal model, and describing function method. A Buck converter with PWM modulation and voltage-mode control is taken as an example to compare the advantages and disadvantages of different methods through simulation analysis. Moreover, the corresponding equivalent circuit with an intuitive physical meaning of state-space average model, generalized average model, and averaged small-signal model is given. The results point out that the generalized average model can improve the modeling accuracy based on the state-space average model. In the linearization techniques, the averaged small-signal model reflects accuracy at low frequencies, but introduces phase lag in the high-frequency region. The describing function method is derived from harmonic linearization, which takes into account the sideband effect and improves the modeling accuracy at high frequencies.

Keywords: State-space average model, generalized average model, linearization techniques, averaged small-signal model, describing function method

1 Introduction

Modeling approaches are the basis to study the characteristics and control approaches of power converters. A power converter with PWM modulation is a switching system with nonlinear and time-varying characteristics. In view of this characteristics, many studies have been performed on its modeling approaches and system analysis in academia and industry. Generally, there are two ways to deal with the time-varying dynamics of converters. One way is to model the converter as a discrete system, and the other way is to model the converter as a continuous system. This paper reviews and compares the commonly used continuous modeling approaches to analyze power converters^[1-3].

The average modeling approaches are widely used to average out the switching dynamics in power converters. Some of the utility of the average

modeling approaches for simulation purposes, using dedicated software products such as SPICE®, SABER®, and MATLAB®, has also been widely proved^[1]. Wester et al.^[4] first proposed a modeling method based on the concept of the circuit average. One of the most representative average modeling approaches is the state-space average model, which was introduced by Middlebrook et al.^[5] in 1976. The state-space averaged model has been shown to have limited utility for stability prediction when the feedback signals have high switching-frequency ripple, such as in the case of peak-current control^[6] and state feedback control^[7-8]. Chetty^[9] proposed the current injected equivalent circuit approach to model switching DC-DC converters. Czarkowski et al.^[10] used the energy conservation method to model the DC-DC converter by considering the power loss. In order to consider the switching ripple, some extended methods appear. Krein et al.^[11-12] developed the Krylov-Bogoliubov-Mitropolsky (KBM) method according to the approximation method by discontinuity points. Sanders et al.^[13-14] proposed generalized average modeling method based on

Manuscript received September 10, 2020; revised October 14, 2020; accepted February 24, 2021. Date of publication March 31, 2021; date of current version March 4, 2021.

* Corresponding Author, E-mail: ljhang@hdu.edu.cn

* Supported by the National Natural Science Foundation of China (51777049, 51707051).

Digital Object Identifier: 10.23919/CJEE.2021.000002

Fourier analysis. These approaches not only can improve the modeling accuracy, but also can be applied to the resonant converter [14]. However, the achieved model is usually complicated and cannot be used in engineering design. These extended methods focus on the approximation of the original system equation of state and have a complete mathematical structure.

Linearization technology generally refers to a nonlinear system near a given steady operating point with small-signal disturbances, just as in the averaged small-signal model [15-16]. The averaged small-signal model is a good tool for practical controller design for industrial and engineering application. However, this model ignores the switching ripple effect and introduces phase lag in the high-frequency region. Therefore, the averaged small-signal model has been shown to have limited utility for stability prediction when the feedback signals have high switching-frequency ripple [17-18].

In addition, the describing function method is recently developed. In the early stage, Middlebrook et al. [19-20] studied the frequency characteristics of current-mode controlled switching converters based on the modeling idea of averaging the inductor current in a switching cycle, but they failed to accurately predict the sub-harmonic oscillation of the system. On this basis, Ridley [21] considered the influence of the sample hold link in the peak current control to obtain an improved average model. Ref. [22] established a multi-frequency model based on the analysis of the nonlinear characteristics of the pulse width modulator, considering the voltage outer loop and ignoring the sideband frequency effect of the inductor current. Aiming at the problem that the improved average model cannot accurately model the frequency conversion control. Yan et al. [23-25] proposed a modeling method based on the described function and obtained the equivalent circuit model with the improved three-terminal switch model on this basis. The model can be used to reveal the high-frequency information of the switching converter with V^2 control [26-27]. This is used to model the LLC converter to obtain the small-signal model according to the basic circuit equation and harmonic balance principle [28-30].

The paper is organized as follows. Section 2 discusses the operating state of the power converters with different switching state by using the switching

function. Section 3 introduces the average modeling methods and limitations of the state-space average model, generalized average model. Section 4 demonstrates the average small-signal model and Section 5 introduces the describing function method. Finally, the four discussed types of models are compared with each other and the conclusion of this paper is given in Section 6.

2 State equation of a switching power converter

In order to describe the modeling methods of converter system, a closed-loop voltage-mode controlled continuous conduction mode (CCM) Buck converter with PWM modulation is selected as an example. The topology of converter is shown in Fig. 1. The parameters of the power stage and controller are summarized in Tab. 1.

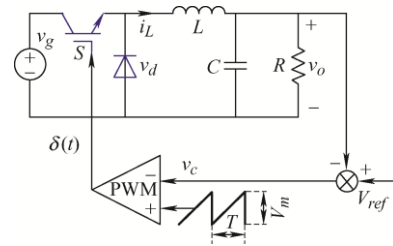


Fig. 1 Voltage mode controlled Buck converter

Tab. 1 Power stage parameters

Parameter	Value
Input voltage v_g/V	12
Output voltage v_o/V	8
Filter inductance L/mH	1
Filter capacitance $C/\mu F$	50
Load resistance R/Ω	10
PWM carrier amplitude V_m/V	1
Switching frequency f_s/kHz	100

As can be seen from Fig. 1, in a switching period T and duty ratio d of the converter, there are two working states of the system. The working states are driven by signal $\delta(t)$, called the switching function, which is

$$\delta(t) = \begin{cases} 0 & 0 \leq t \leq t_{on} \\ 1 & t_{on} \leq t \leq T \end{cases} \quad (1)$$

When the duty ratio $d = t_{on}/T$ (T is the switching period) is constant, the waveform of the switch function is as shown in Fig. 2.

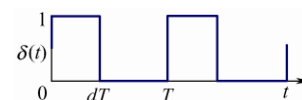


Fig. 2 The waveform of the switch function

According to the switch function $\delta(t)$, there are two states when the switch works in on and off states respectively. Selecting filter inductance current i_L and output voltage v_o as state variables, the state equation of the power stage can be expressed as

$$\begin{cases} L \frac{di_L(t)}{dt} = \delta(t) \cdot v_g(t) - v_o(t) \\ C \frac{dv_o(t)}{dt} = -\frac{v_o(t)}{R} + i_L(t) \end{cases} \quad (2)$$

The state Eq. (2) is a time-varying and discontinuous system. Due to the existence of the switching function, the system cannot be directly applied to the closed-loop controller design. Therefore, some equivalent methods should be applied to obtain the system's small-signal model so that the feedback system controller can be designed.

3 Average modeling approaches

Generally, in order to provide good performance of the system, the control laws need to be designed, then the discontinuous system needs to be converted to a continuous system. Furthermore, it is desired to obtain a model that is easy to use^[1]. For this reason, the average modeling methods are proposed.

3.1 State-space average model

State-space average model was widely used in modeling of PWM converters. However, this modeling method needs to operate under the conditions of low frequency, small ripple, and small-signal hypothesis^[4]. The moving-average operator is a useful tool to eliminate the switching ripple. x is defined as the state valuable. Then the average value of x in each witching period by using the average operator can be expressed as

$$\langle x \rangle(t) = \frac{1}{T} \cdot \int_{t-T}^t x d\tau \quad (3)$$

A generic power electronic converter is described as a dynamic system

$$\frac{d}{dt} x(t) = A_n \cdot x(t) + B_n \cdot \delta(t) \cdot v_g \quad (4)$$

where A_n is input state variable coefficient matrix and B_n is output state variable coefficient matrix. Applying the moving average operator to the dynamic system in Eq. (4), the state-space average model of the power

converter can be summarized as follows through the above examples

$$\begin{cases} \frac{d\langle x \rangle_T(t)}{dt} = A_{av} \langle x \rangle_T(t) + B_{av} v_g \\ A_{av} = \sum_{n=1}^m d_n A_n \\ B_{av} = \sum_{n=1}^m d_n B_n \end{cases} \quad (5)$$

where m is the number of topology changes in a switching period. According to Eq. (5), the state-space average model of nonlinear switching function $\delta(t)$ can be expressed as the duty ratio d . Applying Eq. (5) to the Buck converter state equation in Eq. (2), the matrix parameters can be expressed as

$$\begin{cases} x(t) = \begin{bmatrix} i_L \\ v_o \end{bmatrix} & A_1 = A_2 = \begin{bmatrix} 0 & -\frac{1}{L} \\ \frac{1}{C} & -\frac{1}{RC} \end{bmatrix} & B_1 = \begin{bmatrix} \frac{1}{L} \\ 0 \end{bmatrix} \\ B_2 = \begin{bmatrix} 0 \\ 0 \end{bmatrix} & A_{av} = \begin{bmatrix} 0 & -\frac{1}{L} \\ \frac{1}{C} & -\frac{1}{RC} \end{bmatrix} & B_{av} = \begin{bmatrix} d \\ L \\ 0 \end{bmatrix} \end{cases} \quad (6)$$

The model in Eq. (5) is the analytical approach, which cannot directly express the physical meaning of the circuit^[5]. Therefore, the equivalent circuit topological diagram, as shown in the Fig. 3, where the coupling terms are emphasized and from which a power converter equivalent model can also be obtained, is established.

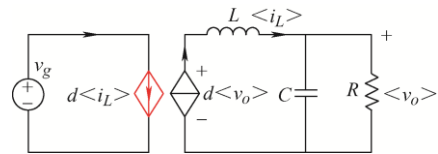


Fig. 3 Average model equivalent circuit of Buck converter

Therefore, the waveform curve of the average model can be calculated by the equivalent circuit or the state-space average equation directly. Fig. 4 presents a comparison between the detailed switching converter and the averaged behavior of the converter, and the time evolution of state variables, i.e., the inductor current i_L and output voltage v_o , are shown.

Among the advantages of the state-space average model, in particular is the ease of building and implementing the model and ability to assess the dynamic characteristics. Besides, the model is not useful for resonant converters.

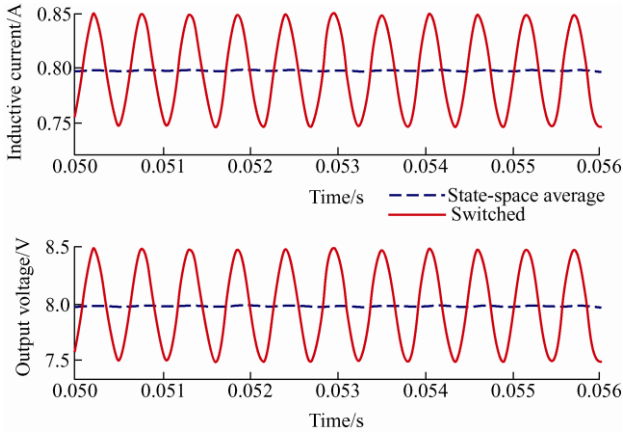


Fig. 4 The simulation waveform of the output voltage and inductance current: State-space average model and detailed switching converter

3.2 Generalized average model

To consider the switching ripple effect, Prof. George Verghese from Massachusetts Institute of Technology (MIT) proposed generalized average model based on Fourier analysis [13-14]. The generalized average model is a more ideal modeling method than the state-space average model. This model can approximate the time-domain model to the required accuracy and can accurately analyze the transient process of power converters.

The core idea of the generalized average model is to describe the periodic signal in the time domain by using Fourier series and linearize the nonlinear part. Therefore, the periodic variable $x(t)$ can be expressed as

$$x(\tau) = \sum_{-\infty}^{\infty} \langle x \rangle_k(t) \exp(jk\omega\tau) \quad (7)$$

where $\omega = 2\pi f_s$ is the fundamental pulsation and $\langle x \rangle_k(k)$ is the Fourier coefficient of the k th component, which is given by

$$\langle x \rangle_k(t) = \frac{1}{T} \int_{t-T}^t \langle x \rangle_k(\tau) \exp(-jk\omega\tau) d\tau \quad (8)$$

Because k represents a harmonic component, the modeling result will be more accurate as k increases. However, this greatly increases the amount of calculations. Fig. 5 shows the Eq. (8) applied to the switching function $\delta(t)$ with different Fourier series. Modeling results become much more accurate when more harmonics are involved.

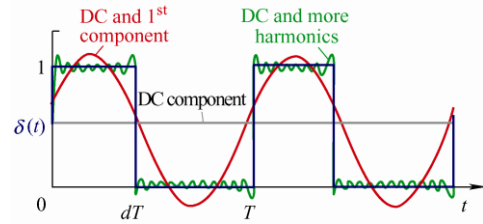


Fig. 5 Different Fourier-series harmonic component of the switch function

Applying the Fourier series Eq. (8) to Eq. (2), the generalized average model of Buck converter can be expressed as

$$\begin{cases} \frac{d\langle i_L \rangle_k(t)}{dt} = \frac{1}{L} (v_g \langle \delta \rangle_k(t) - \langle v_o \rangle_k(t)) - jk\omega \langle i_L \rangle_k(t) \\ \frac{d\langle v_o \rangle_k(t)}{dt} = \frac{1}{C} \left(\langle i_L \rangle_k(t) - \frac{\langle v_o \rangle_k(t)}{R} \right) - jk\omega \langle v_o \rangle_k(t) \end{cases} \quad (9)$$

For calculation convenience, most existing literature chooses the DC component and the first-order harmonic component [13], that is, the cases of $k=0$ and $k=1$ are considered. Similarly, by applying discrete convolution and conjugation properties to Eq. (9), the generalized average model can be got through the state equation expressions of DC component and first-order harmonic component. Afterwards, an analytical solution can be obtained by solve the two state equations to obtain [14], which will not be detailed here.

The equivalent circuit of the first-order harmonic component Eq. (9) can be obtained, as shown in Fig. 6.

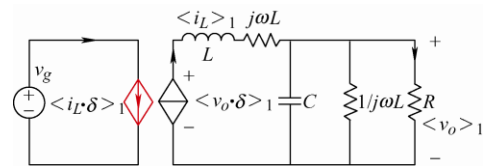


Fig. 6 Equivalent diagram of first-order harmonic component of Buck converter

From the first-order harmonic component results, as shown in Fig. 6, the AC impedances are emphasized. One need only write Kirchoff's equations by using Fig. 6 to obtain the analytical model equal to Eq. (9) and finalize the computation by calculating the real and imaginary parts of the complex variables to obtain the generalized average model final form of the Buck converter. The results of applying the generalized average model to the the Buck converter topology are shown in Fig. 7.

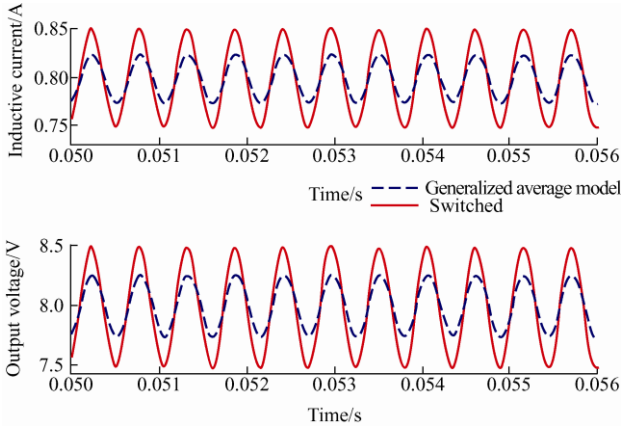


Fig. 7 The simulation waveform of the output voltage and inductive current: generalized average model and detailed switching converter

The simulation results show that the generalized average model is characterized by considering the AC characteristics of the switching system. Therefore, its order is higher than that of the average model, and its accuracy is higher. However, because this method only considers some harmonic components and fails to reflect all AC characteristics, its accuracy and complexity need to be considered comprehensively.

4 Averaged small-signal model

In order to complete the feedback control design of the converter system using the classical control theory of linear systems, it is necessary to further adopt the small-signal perturbation method to linearize the above nonlinear equation near a given static operating point [2].

The averaged small-signal model is based on the small-signal perturbation method to linearize the nonlinear equation near a static operating point. The converter is assumed to work at a certain steady-state operating point with the duty cycle D , inductor current I_L , input voltage V_g and output voltage V_o . For the average model of Buck converter, supposing a low-frequency small disturbance near the steady-state operating point gives

$$\begin{cases} d(t) = D + \hat{d}(t) & v_g(t) = V_g + \hat{v}_g(t) \\ v_o(t) = V_o + \hat{v}_o(t) & i_L(t) = I_L + \hat{i}_L(t) \end{cases} \quad (10)$$

The averaged small-signal model of the Buck converter can be rewritten as

$$\begin{cases} L \frac{d\hat{i}_L(t)}{dt} = V_g \cdot \hat{d}(t) + D \cdot \hat{v}_g(t) - \hat{v}_o(t) \\ C \frac{d\hat{v}_o(t)}{dt} = -\frac{\hat{v}_o(t)}{R} + \hat{i}_L(t) \end{cases} \quad (11)$$

Similarly, a more intuitive small-signal equivalent circuit model can be established according to the average small-signal model, which provides convenience for analyzing the small-signal characteristics of the converter. Fig. 8 shows a small-signal equivalent circuit of the Buck converter.

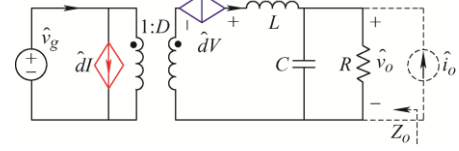


Fig. 8 The small-signal equivalent circuit of the Buck converter

Fig. 8 intuitively reflects the small-signal treating processes of the Buck converter. To further analyze the low frequency dynamic characteristics of the converter, the input-output transfer function G_{vg} , the control-output transfer function G_{vd} , and the output impedance Z_o , can be derived as follows

$$\begin{cases} G_{vg}(s) = \left. \frac{\hat{v}_o(s)}{\hat{v}_g(s)} \right|_{\hat{d}=0} \\ G_{vd}(s) = \left. \frac{\hat{v}_o(s)}{\hat{d}(s)} \right|_{\substack{\hat{i}_L=0 \\ \hat{v}_g=0}} \\ Z_o(s) = \left. \frac{\hat{v}_o(s)}{\hat{i}_o(s)} \right|_{\hat{d}=0} \end{cases} \quad (12)$$

In addition, it is known that the input perturbation of the PWM comparator varies slowly compared with the switching frequency [5]. So, the transfer function of the PWM comparator can be expressed as

$$G_{PWM} = \frac{1}{V_M} \quad (13)$$

Therefore, the control system block diagram of the average small-signal model for a voltage mode controlled Buck converter can be obtained, as shown in Fig. 9.

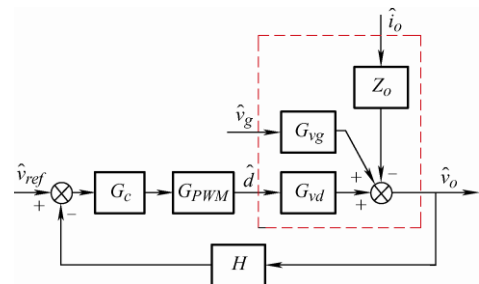


Fig. 9 The control system block diagram for voltage-mode controlled Buck converter

According to Fig. 9, the loop gain of the voltage mode controlled switching converter can be obtained

$$T(s) = G_c(s)G_{vd}(s)G_{PWM}H(s) \quad (14)$$

where $G_c(s)$ is the compensator with a PI controller and $H(s)$ is the feedback [7]. The closed-loop feedback control, input-output, output impedance, and output impedance closed-loop transfer function are expressed as

$$\begin{cases} \frac{\hat{v}_o(s)}{\hat{v}_g(s)} = \frac{G_{vg}(s)}{1+T(s)} \\ \frac{\hat{v}_o(s)}{\hat{d}(s)} = \frac{G_{vd}(s)}{1+T(s)} \\ \frac{\hat{v}_o(s)}{\hat{i}_o(s)} = \frac{Z_o(s)}{1+T(s)} \end{cases} \quad (15)$$

The above formula shows that the influence of the input voltage or load disturbance on the output voltage can be effectively suppressed by increasing the loop gain $T(s)$. Fig. 10 shows the frequency response of the loop gain of a voltage-mode controlled Buck converter.

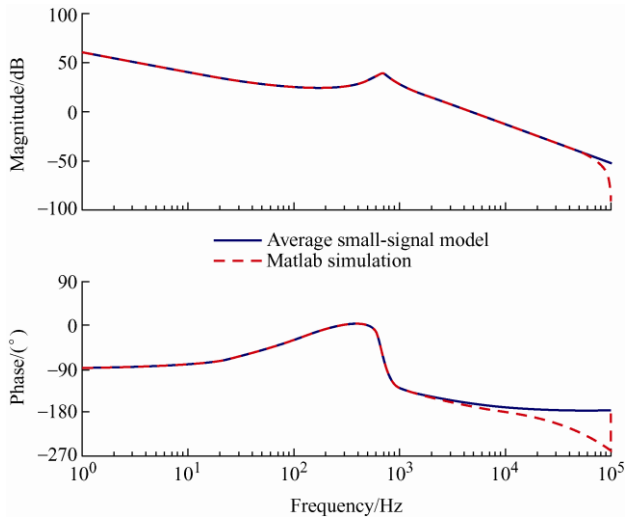


Fig. 10 Loop gain of a voltage mode controlled Buck converter

Obviously, the averaged small-signal model introduces phase lag in the high-frequency region. The averaged small-signal model eliminated the switching ripple effect and the modeling results is questionable at high frequencies because of linearization and time-invariant assumptions, so it can only extract the low-frequency small-signal characteristics of the system.

5 Describing function method

It is known that the switching devices in the power converter and the PWM link in the control loop make the system exhibit nonlinear characteristics [2]. When a small-signal disturbance with frequency f_x is injected into the input voltage $v_g(t)$ and modulation link $v_c(t)$, the switching network output voltage $v_d(t)$ and switching function $\delta(t)$ not only contain disturbance frequency components [20], but also are affected by the sideband effect shown in Fig. 11.

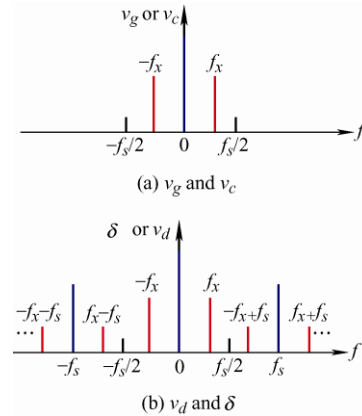


Fig. 11 Sideband effect generated by the switching frequency domain waveforms

Fig. 12 reveals the multi-frequency characteristics of the voltage mode controlled Buck converter from the perspective of the frequency domain. Therefore, it is necessary to consider the sideband effect in the system. The diagram becomes the small-signal averaged model in Fig. 8 if only the perturbation frequency component (marked by bold blue lines) is involved in the modeling.

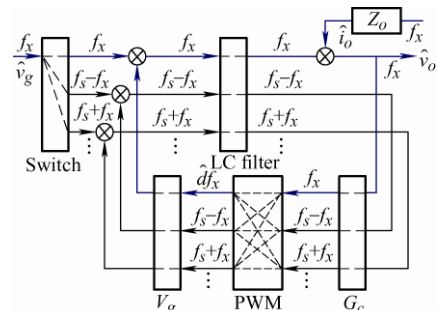


Fig. 12 Multi-frequency input and multi-frequency output relationship of closed-loop controlled switching converter

The error of the small-signal average modeling method at high frequencies is mainly due to the sideband effect of the switching modulation. In order

to improve the accuracy of modeling, some frequency-domain modeling methods considering the sideband effect are proposed, among which, the describing function method provides an effective solution for modeling the sideband effect^[23].

The essence of the describing function method is a harmonic balance method based on Fourier series. Generally, if the input to a nonlinear system is a sinusoidal function

$$u(t) = U \sin \omega t \quad (16)$$

the output of the system can be expressed as

$$y(t) = \frac{A_0}{2} + \sum_{k=1}^{\infty} A_k \sin k\omega t + \sum_{k=1}^{\infty} B_k \cos k\omega t = \frac{A_0}{2} + \sum_{k=1}^{\infty} Y_k \sin(k\omega t + \phi_k) \quad (17)$$

where

$$\begin{cases} A_k = \frac{1}{\pi} \int_0^{2\pi} y(t) \cdot \cos k\omega t \cdot dt \\ B_k = \frac{1}{\pi} \int_0^{2\pi} y(t) \cdot \sin k\omega t \cdot dt \\ Y_k = \sqrt{A_k^2 + B_k^2} \\ \phi_k = \arctan \frac{A_k}{B_k} \end{cases} \quad (18)$$

When a disturbance with frequency $f_x = \omega/2\pi$ occurs, the describing function expression of the input and output at the disturbance frequency is as follows

$$G = \frac{Y_1}{U} \angle \phi_1 = \frac{\sqrt{A_1^2 + B_1^2}}{U} \angle \arctan \frac{A_1}{B_1} \quad (19)$$

In voltage mode controlled Buck converters, a describing function method is proposed to explain the measured phase delay of the loop gain by considering the sideband effect of PWM comparator^[26], which is

$$T_{df}(f_x) = \frac{T_{av}(f_x)}{1 + T_{av}(f_x - f_s)} \quad (20)$$

where $T_{df}(f_x)$ is the loop gain of a voltage mode controlled Buck converter. The influence from the sideband effect is shown in the denominator. According to the previous analysis, the sideband effect has a greater impact on the high-frequency range.

Fig. 13 shows a bode diagram of the loop gains of a closed loop controlled Buck converter obtained by simulation. Compared with the average small-signal model, the describing function method considers the influence of sideband effect from the perspective of the frequency domain, so it improves the accuracy of

the model. Therefore, for stability analysis at high-frequency cases, it is necessary to use the describing function method to replace the average model.

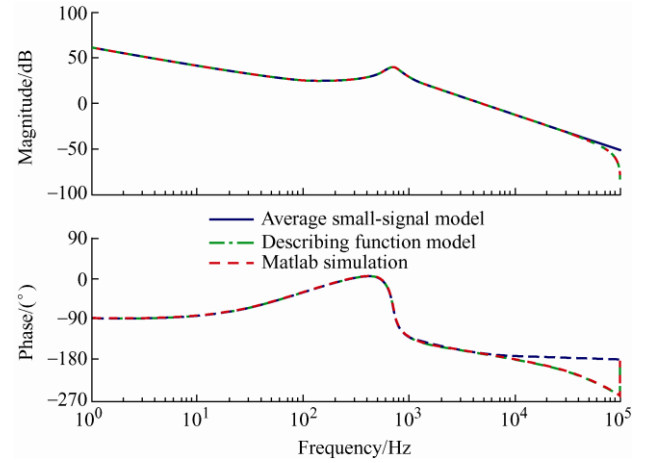


Fig. 13 Loop gain of a voltage mode controlled Buck converter

The describing function method has been developed recently. Another application of the describing function method is to analyze the small-signal model of the resonant converter because when many inverters are connected to the AC grid, the describing function method can be used to analyze the small-signal model of the resonant inverter^[30] and LLC resonant^[29] converter system. The nonlinear part of the resonant converter is approximately linearized by using the principle of extended describing function. After that, the small-signal model of the resonant converter can be obtained according to the basic circuit equation and harmonic balance principle^[28].

6 Conclusions

The modeling methods of power electronic converters are the theoretical basis of switching power design. Existing modeling methods are numerous and lack overall introductions. This paper systematically classifies and summarizes various modeling methods in continuous mode, and the comparison results of different modeling methods are listed in Tab. 2. Moreover, the corresponding equivalent circuit with an intuitive physical meaning of the state-space average model, generalized average model, and averaged small-signal model is given. Through this paper, researchers and engineers may gain a comprehensive understanding of the modeling theory. Thus, effective design guidelines can be selected quickly for different kinds of converters.

Tab. 2 Comparison of different modeling methods

Model name	Model accuracy	Model complexity	Main application areas
State-space average model	Low accuracy	Low	Simulation and large-signal analysis
Generalized average model	Medium accuracy	Medium	Simulation and large-signal analysis
Averaged small-signal model	Low-frequency accuracy	Low	Controller design and stability analysis
Describing function method	Both low-and high-frequency accuracy	High	Loop gain phase delay and subharmonic oscillation

One of the advantages of the state-space average model is that it is easy to establish and implement, and it has good approximation accuracy when predicting low-frequency information. In contrast, when high-frequency information cannot be ignored, the accuracy of the model begins to decline. In addition, the model is not useful for resonant converters.

The generalized average model proves to be a more accurate model than the state-space average model because the switching ripple is considered. However, due to the increase in state variables, the complexity of the system also increases.

The averaged small-signal model is a good tool for engineering controller design. However, this model ignores the switching ripple effect and introduces phase lag in the high-frequency region.

The describing function method can accurately predict the sub-harmonic oscillation in the switching power supply due to the influence of the sideband frequency, and it can accurately analyze the frequency-domain characteristics of the constant-frequency (PWM and phase shift) or variable-frequency power converter, but the modeling process of the describing function method is more complicated.

The above modeling methods have their respective advantages and disadvantages. In general, a tradeoff should be made in terms of modeling accuracy and calculation complexity.

References

- [1] R W Erickson, D Maksimović. Fundamentals of power electronics. 2nd ed. New York: Springer, 2001.
- [2] J Kassakian, M Schlecht, G Verghese. Principles of power electronics. 1st ed. Reading: Addison-Wesley, 1991.
- [3] F Blaabjerg, Y Yang, D Yang, et al. Distributed power-generation systems and protection. *Proceedings of the IEEE*, 2017, 105(7): 1311-1331.
- [4] G W Wester, R D Middlebrook. Low-frequency characterization of switched DC-DC converters. *IEEE Transactions on Aerospace and Electronic Systems*, 1973, 9(3): 376-385.
- [5] R D Middlebrook, S Cuk. A general unified approach to modeling switching converter power stages. *International Journal of Electronics*, 1976, 42(6): 521-550.
- [6] X Yue, X Wang, F Blaabjerg. Review of small-signal modeling methods including frequency-coupling dynamics of power converters. *IEEE Transactions on Power Electronics*, 2019, 34(4): 3313-3328.
- [7] Z Y Guo, H Li, C Liu, et al. Stability-improvement method of cascaded DC-DC converters with additional voltage-error mutual feedback control. *Chinese Journal of Electrical Engineering*, 2019, 5(2): 63-71.
- [8] M Andresen, J Kuprat, V Raveendran, et al. Active thermal control for delaying maintenance of power electronics converters. *Chinese Journal of Electrical Engineering*, 2018, 4(3): 13-20.
- [9] P R K Chetty. Modelling and analysis of cuk converter using current injected equivalent circuit approach. *IEEE Trans. Ind. Electron.*, 1983, 30(1): 56-59.
- [10] D Czarkowski, M K Kazimierczuk. Energy-conservation approach to modeling PWM DC-DC converters. *IEEE Transactions on Power Electronic*, 1993, 29(3): 1059-1063.
- [11] P T Krein, J Bentsman, R M Bass, et al. On the use of averaging for the analysis of power electronic systems. *IEEE Transactions on Power Electronic*, 1990, 5(2): 182-190.
- [12] R M Bass, B Lehman. Switching frequency dependent averaged models for PWM DC-DC converters. *IEEE Transactions on Power Electronics*, 1996, 11(1): 89-98.
- [13] S R Sanders, J M Noworolski, G C Verghese, et al. Generalized averaging method for power conversion

- circuits. *IEEE Transactions on Power Electronic*, 1991, 6(2): 251-259.
- [14] V A Caliskan, G C Verghese, A M Stankovic. Multi-frequency averaging of DC/DC converters. *IEEE Transactions on Power Electronic*, 1999, 14(1): 124-133.
- [15] J Yao, K Zheng, A Abramovitz. Small-signal model of switched inductor boost converter. *IEEE Transactions on Power Electronic*, 2019, 34(5): 4036-4040.
- [16] A Ayachit, M K Kazimierczuk. Averaged small-signal model of PWM DC-DC converters in CCM including switching power loss. *IEEE Transactions on Circuits and Systems II: Express Briefs*, 2019, 66(2): 262-266.
- [17] J Sun, Y Qiu, M Xu, et al. High-frequency dynamic current sharing analyses for multiphase buck VRs. *IEEE Transactions on Power Electronic*, 2007, 22(6): 2424-2431.
- [18] Y Qiu, M Xu, J Sun, et al. A generic high-frequency model for the nonlinearities in buck converters. *IEEE Transactions on Power Electronic*, 2007, 22(5): 1970-1977.
- [19] R D Middlebrook. Modeling current-programmed buck and boost regulators. *IEEE Transactions on Power Electronic*, 1989, 4(5): 36-52.
- [20] F D Tan, R D Middlebrook. Unified modeling and measurement of current-programmed converters. *Power Electronics Specialists Conference, Washington, USA: IEEE*, 1993: 380-387.
- [21] R B Ridley. A new, continuous-time model for current-mode control. *IEEE Transactions on Power Electronic*, 1991, 6(2): 271-280.
- [22] Y Qiu, M Xu, K Yao, et al. Multi-frequency small-signal model for Buck and multi-phase Buck converters. *IEEE Transactions on Power Electronics*, 2006, 21(5): 1185-1192.
- [23] Y Yan, F C Lee, P Mattavelli. Analysis and design of average current mode control using a describing-function-based equivalent circuit model. *IEEE Transactions on Power Electronic*, 2013, 28(10): 4732-4741.
- [24] J Li, F C Lee. New modeling approach and equivalent circuit representation for current mode control. *IEEE Transactions on Power Electronic*, 2010, 25(5): 1218-1230.
- [25] Y Yan, F C Lee, P Mattavelli. Unified three-terminal switch model for current mode controls. *IEEE Transactions on Power Electronic*, 2012, 27(9): 4060-4070.
- [26] Y Yan, F C Lee, P Mattavelli, et al. Small signal analysis of V^2 control using equivalent circuit model of current mode controls. *IEEE Transactions on Power Electronic*, 2016, 31(7): 5344-5353.
- [27] S Tian, F C Lee, Q Li, et al. Unified equivalent circuit model and optimal design of V^2 controlled buck converters. *IEEE Transactions on Power Electronic*, 2016, 31(2): 1734-1744.
- [28] M P Foster, C R Gould, A J Gilbert, et al. Analysis of CLL voltage-output resonant converters using describing functions. *IEEE Transactions on Power Electronic*, 2008, 23(4): 1772-1781.
- [29] S Tian, F C Lee, Q Li. Equivalent circuit modeling of LLC resonant converter. *IEEE Transactions on Power Electronic*, 2020, 35(8): 8833-8845.
- [30] Z Ye, P K Jain, P C Sen. Phasor-domain modeling of resonant inverters for high-frequency AC power distribution systems. *IEEE Transactions on Power Electronic*, 2009, 24(4): 911-924.



Dong Yan received his B.S. degree from the School of Electrical Engineering, Henan University of Technology, Zhengzhou, China, in 2018. He is currently working towards his Ph.D. degree at the School of College of Automation, Hangzhou Dianzi University, Hangzhou, China. His research interests include modeling and analysis of power electronic systems.



Chenglin Yang is a senior engineer at INVT Power System (Shenzhen) Co., Ltd. His research interest is power electronics.

He obtained his master degree in electrical engineering from Zhejiang University in 2004. Upon attaining his master degree, he joined Emerson Network Power Company, where he held a number of important positions as a software manager.

In 2008, he joined Guangdong East Power Supply Company as R&D director where he led the team to achieve remarkable success. He joined INVT Power System (Shenzhen) Co., Ltd. As chief R&D engineer and deputy general manager in July 2010. He is mainly responsible for products development of UPS.



Lijun Hang received the B.S. and Ph.D. degrees in electrical engineering from Zhejiang University, Hangzhou, China, in 2002 and 2008, respectively. From 2008 to 2011, she was a postdoctoral researcher with Zhejiang University. From 2011 to September 2013, she was a research assistant professor with CURENT, University of Tennessee, Knoxville, TN, USA. From 2013 to 2015, she

was an associate professor at the Department of Electrical Engineering, Shanghai Jiao Tong University, Shanghai, China. Since 2015, she has been a professor at Hangzhou Dianzi University. Her research interests include digital control of power electronics for grid-connected converters, bidirectional DC-DC converters for microgrids, and renewable energy systems. She has authored or co-authored more than 110 published technical papers.



Yuanbin He received the Ph.D. degree in electrical engineering from the City University of Hong Kong, Hong Kong, China, in 2017. He also worked as a research assistant with the City University of Hong Kong from April 2013 to August 2013, and also as a postdoctoral research fellow from February 2017 to July 2017. From July 2011 to March

2013, he worked as an associate researcher with Nanjing FSP-Powerland Technology Inc., Nanjing, China, where he has been involved in research and development of DC-DC and DC-AC converters. From February 2016 to June 2016, he was a visiting scholar at the University of Manitoba, Winnipeg, MB, Canada. Since May 2017, he has been with the Hangzhou Dianzi University, Hangzhou, China, where he is currently a research associate professor with the Department of Electrical Engineering and Automation. His current research interests include renewable energy-generation systems, power quality, and smart grids.



Ping Luo received the B.S. and Ph.D. degrees in electrical engineering from Zhejiang University, Hangzhou, China, in 2000 and 2006, respectively. From 2014 to 2015, she was a research assistant professor with Carnegie Mellon University, USA. Since 2006, she has been an associate professor at Hangzhou

Dianzi University. Her research interests include the energy Internet and smart grid, active distribution network optimization scheduling, and the engineering electromagnetic field inverse problem.



Lei Shen received the B.S. degree and Ph.D. degree in electrical engineering from Zhejiang University, Hangzhou, China, in 2007 and 2012, respectively. From 2012 to 2014, he was a research fellow in the Department of Electrical and Electronic Engineering, The University of Nottingham, Nottingham, UK. He is currently a senior research fellow in the University of Nottingham, Zhejiang, China.

His current research interests include the integration of power electronics with electric machines and power grids.



Pingliang Zeng is a professor at Hangzhou Dianzi University, Hangzhou, China, and a national special expert. He is a Chartered Engineer (CEng), Fellow of the IET, senior member of IEEE, and a member of IEC TC122 and TC8.

He obtained his bachelor and PhD degrees, both in electrical engineering, respectively from Huazhong University of Science and Technology, China, in 1984, and Strathclyde University, UK, in 1990. Upon attaining doctorate degree, he joined National Grid Company (NGC), UK, where he held a number of important positions including system operator incentives and strategy manager, and network design manager.

In 2012, he joined China Electric Power Research Institute as the chief expert in Power System Analysis and Planning, where he led a research team undertaking a number of key projects including National High Technology Development ("863" Plan), SGCC special projects, and key Sino-UK joint research projects funded by National Natural Science Foundation of China on integration of EV and energy storage in power systems. He joined Hangzhou Dianzi University in August 2017. He has published one book and about 100 academic papers.

His current research interest includes power system planning under uncertainty, system operations, renewable energy integration, electric vehicle and energy storage, and multi-energy systems.